Combined DFT and Geometrical-Topological Analysis of Li-ion conductivity in Complex Hydrides

Valerio Gulino[1#], Anna Wolczyk[1#], Andrey A. Golov[2], Roman A. Eremin[2,3], Mauro Palumbo[1], Carlo Nervi[1], Vladislav A. Blatov[2,3*], Davide M. Proserpio[3,4] and Marcello Baricco[1]*

[1]Department of Chemistry and NIS, University of Turin, Via P. Giuria 9, I-10125 Torino, Italy

[2]Samara Center for Theoretical Materials Science, Samara University, Samara 443011, Russia

[3]Samara Center for Theoretical Materials Science, Samara State Technical University, Samara 443100, Russia

[4]Dipartimento di Chimica, Università degli studi di Milano, 20133, Milano, Italy

[#]co-first authors

[*]Corresponding authors:

Prof. Mauro PALUMBO
Department of Chemistry, University of Turin
Via Pietro Giuria, 9 I-10125 TORINO (Italy)
Tel. + 39 011 670 7097 Fax. + 39 011 670 7855
e-mail: mauro.palumbo@unito.it

Prof. Vladislav A. BLATOV
Samara Center for Theoretical Materials Science, Samara State Technical University
Samara 443100, Russia
Tel. +7 846 3356798 Fax: +7 846 2784400
e-mail: blatov@topospro.com

Supporting information

Crystal structure of investigated complex hydrides

Sample	Space Group	Lattice constants (Å)	Ref.
$LiBH_4$	*Pnma*	a = 7.178 Å b = 6.803 Å c = 4.436 Å	1
Li_2NH	*Fm3m*	a = 5.074	2
$LiNH_2$	*I-4*	a = 5.079 c = 10.113	3
$Li_2BH_4NH_2$	*R-3*	a = 14.498 c = 9.248	4
$Li_4BH_4(NH_2)_3$	$I2_13$	a = 10.673	4
$Li_5(BH_4)_3NH$	*Pnma*	a = 10.203, b = 11.501 c = 7.047	5

Table S1. *Structural details of all considered samples.*

Topological analysis

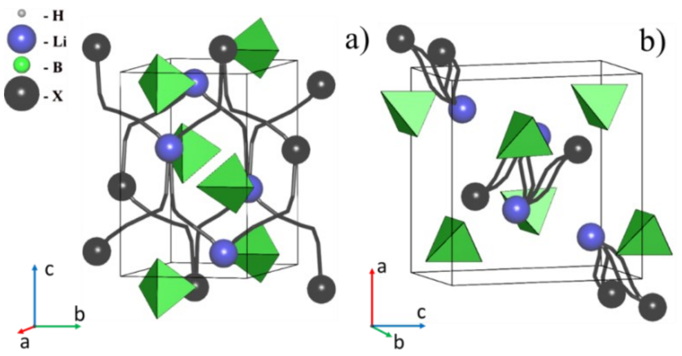

Figure S1. *The lowest energy Li^+ migration pathways in the $LiBH_4$ structure. The migration energies of the pathways: a) 0.242; b) 0.298 eV. Hereafter the points labeled as X correspond to equilibrium Li positions and are linked by the NEB trajectories.*

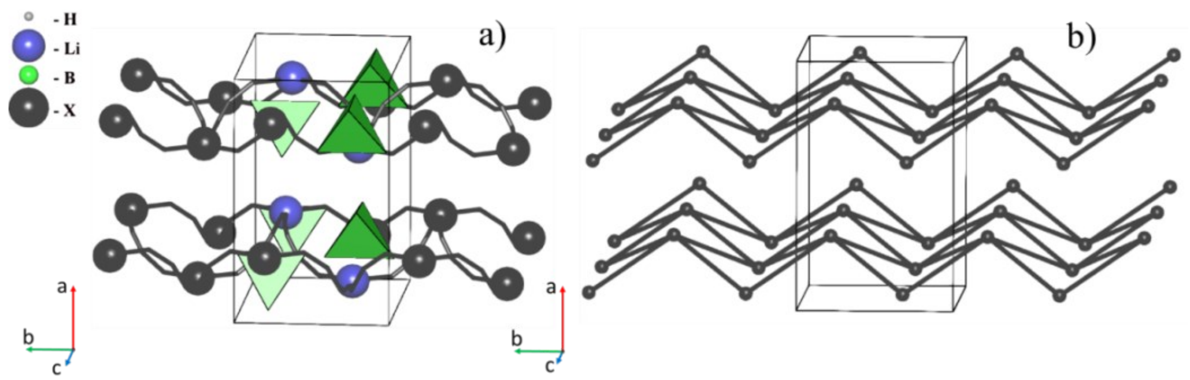

Figure S2. *a) The lowest energy two-periodic Li^+ migration map in the $LiBH_4$ structure, b) the simplified migration map of the sql topology.*

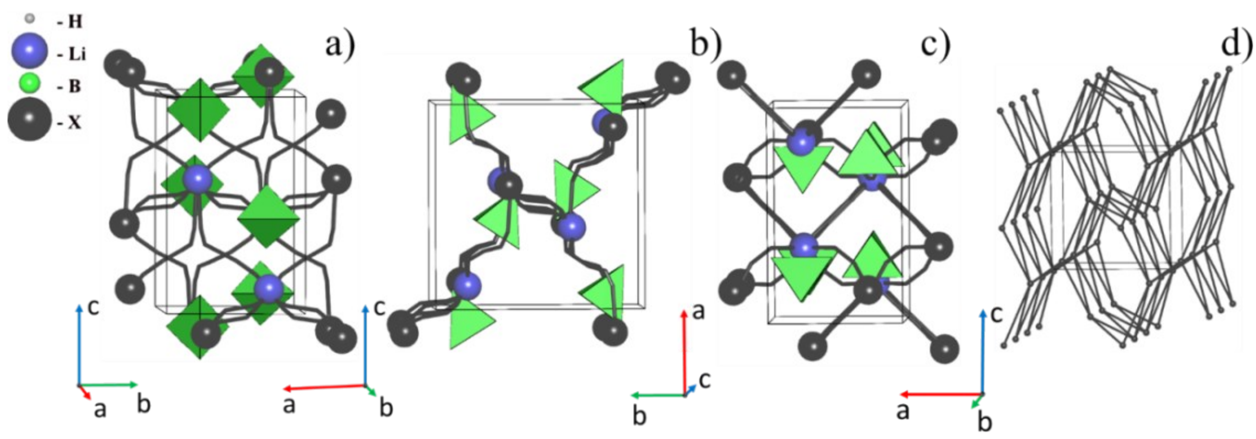

Figure S3. *a)-c) The lowest energy three-periodic Li^+ migration map in the $LiBH_4$ structure, d) the simplified migration map of the acs topology.*

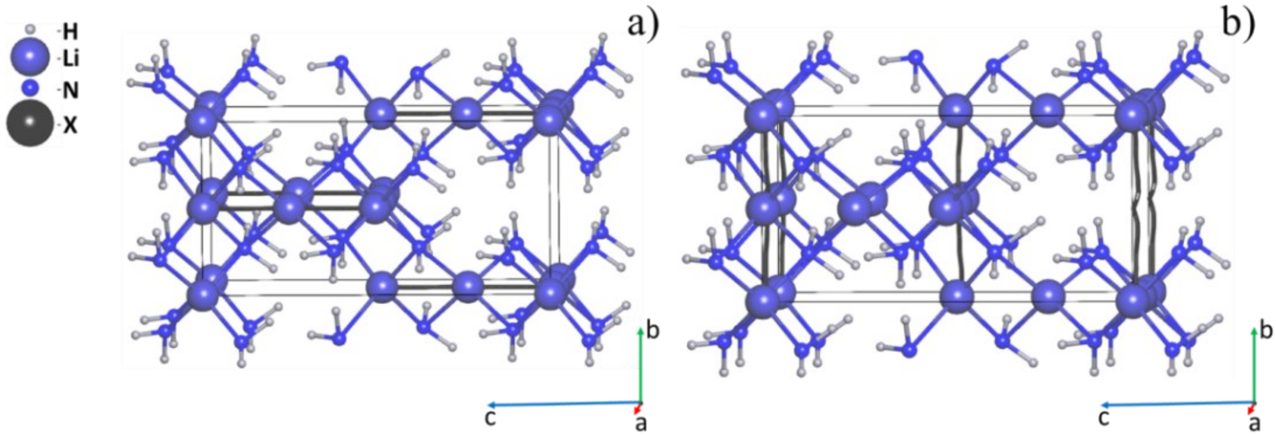

Figure S4. *The lowest energy Li^+ migration pathways in the structure $LiNH_2$. The migration energies of the pathways: a) 0.179; b) 0.461 eV.*

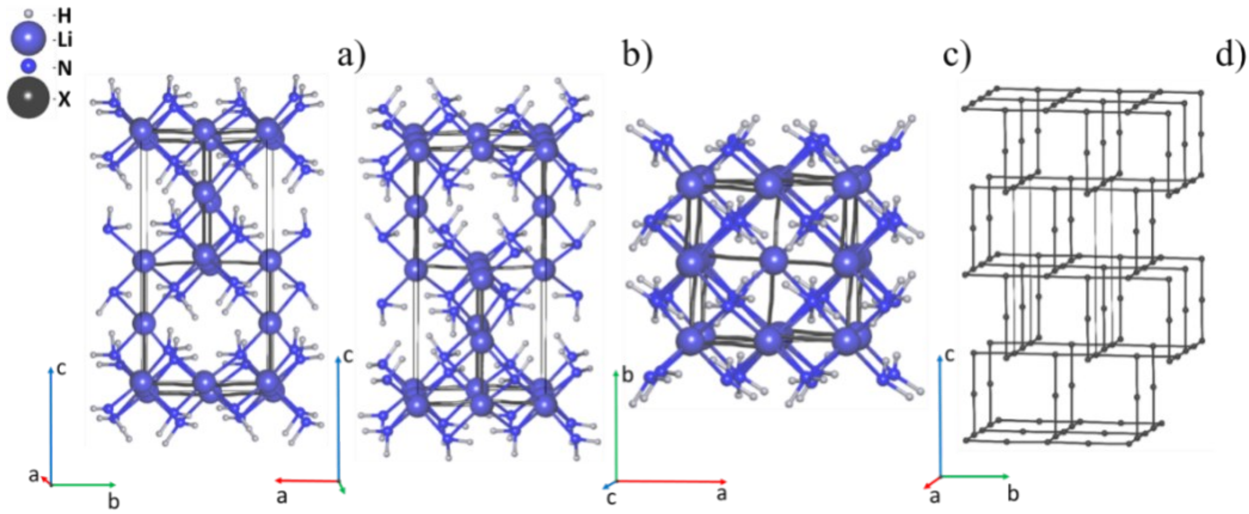

Figure S5. *a)-c) The lowest energy three-periodic Li^+ migration map in the $LiNH_2$ structure, d) the simplified migration map of the tfa topology.*

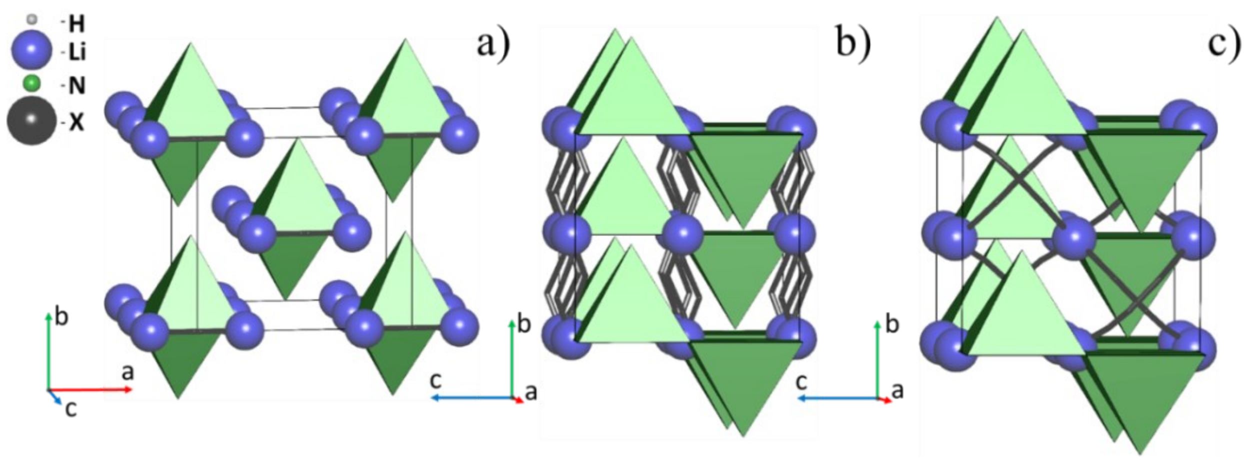

Figure S6. *The lowest energy Li^+ migration pathways in the Li_2NH structure. The migration energies of the pathways: a) 0.007; b) 0.308; c) 0.321 eV.*

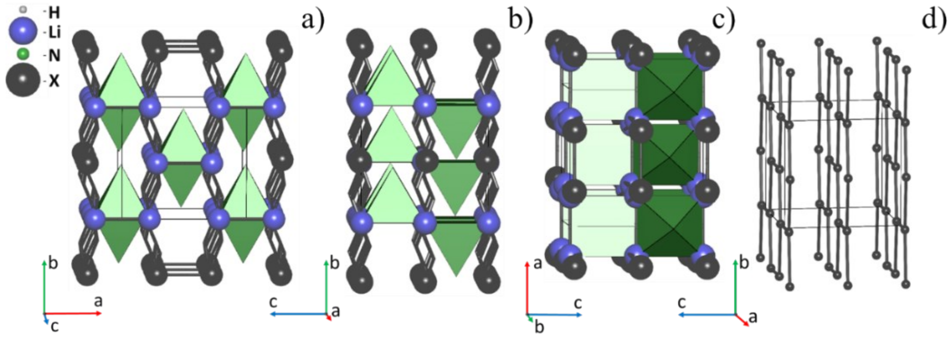

Figure S7. *a)-c) The lowest energy two-periodic Li^+ migration map in the Li_2NH structure, d) the simplified migration map of the hcb topology.*

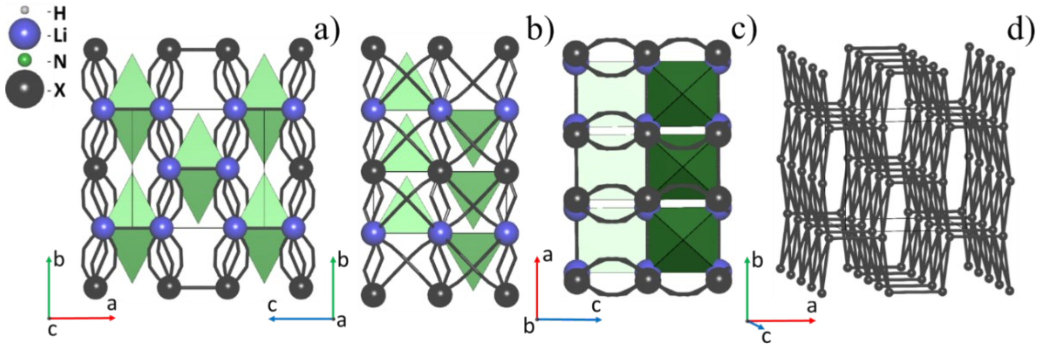

Figure S8. *a)-c) The lowest energy three-periodic Li^+ migration map in the Li_2NH structure, d) the simplified migration map of the sqc2-7-Cmmm topology.*

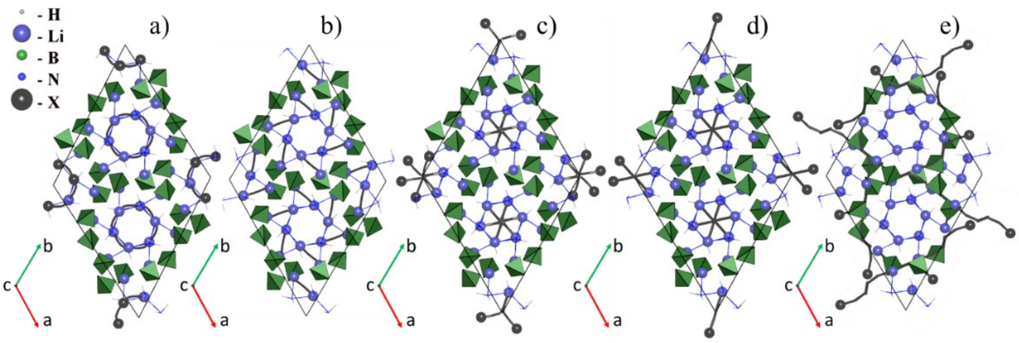

Figure S9. *The lowest energy Li^+ migration pathways in the $Li_2BH_4NH_2$ structure. The migration energies of the pathways: a) 0.176; b) 0.365; c) 0.445; d) 0.481; e) 0.525 eV.*

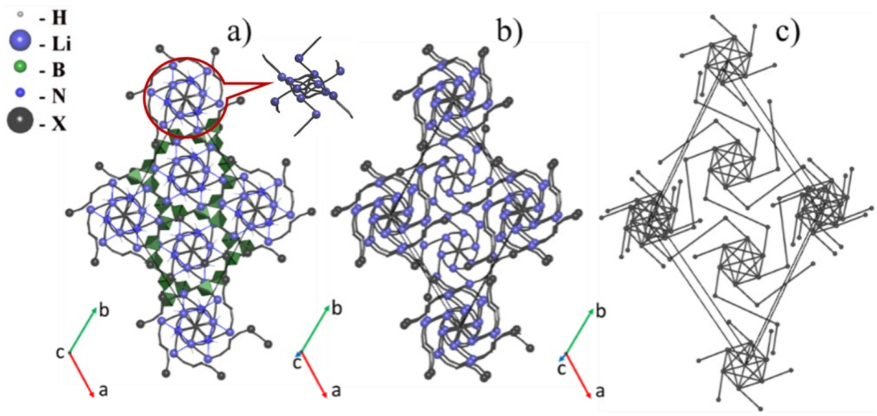

Figure S10. *a), b) The lowest energy three-periodic 2-fold interpenetrated Li^+ migration map in the $Li_2BH_4NH_2$ structure, c) the simplified migration map.*

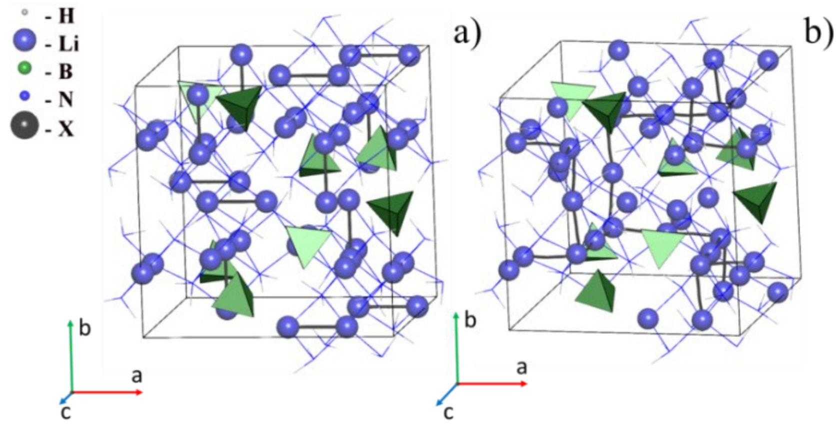

Figure S11. *The lowest energy Li^+ migration pathways in the $Li_4BH_4(NH_2)_3$ structure. The migration energy of the pathways: a) 0.212; b) 0.296 eV.*

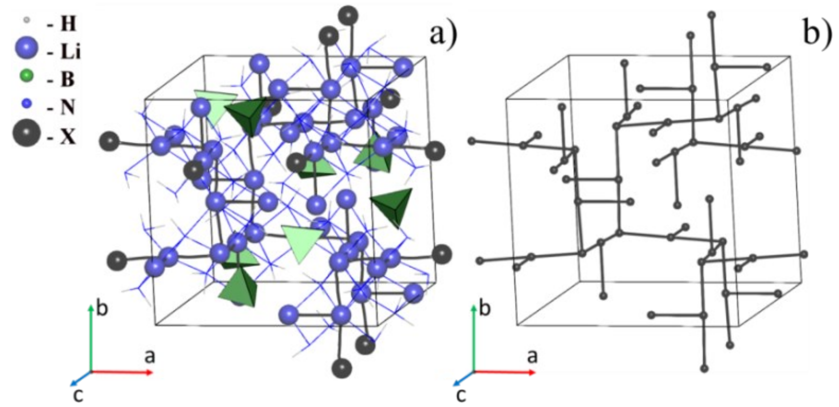

Figure S12. *a) The lowest energy three-periodic Li^+ migration map in the structure $Li_4BH_4(NH_2)_3$, b) the simplified migration map of the srs topology.*

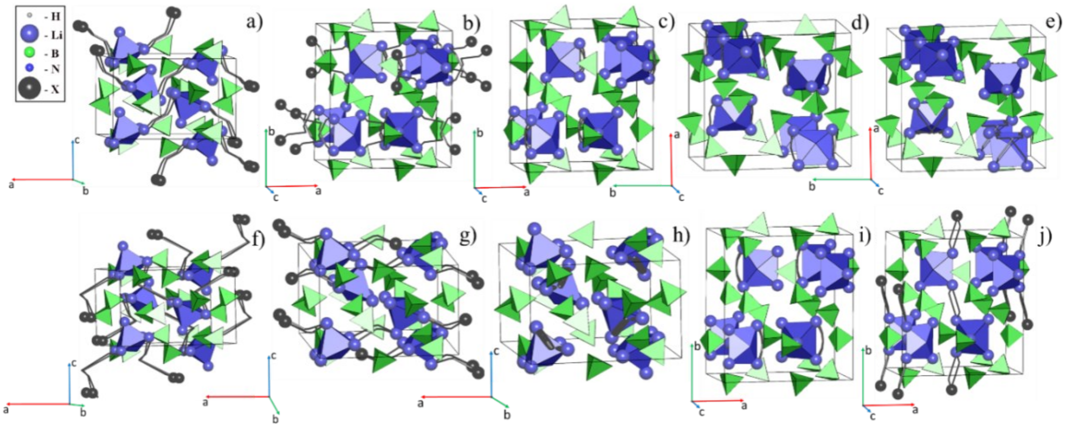

Figure S13. *The lowest energy Li^{+} migration pathways in the $Li_5(BH_4)_3NH$ structure. The migration energies of the pathways: a) 0.237; b) 0.282; c) 0.340; d) 0.397; e) 0.401; f) 0.479; g) 0.536; h) 0.541; i) 0.547; j) 0.559 eV.*

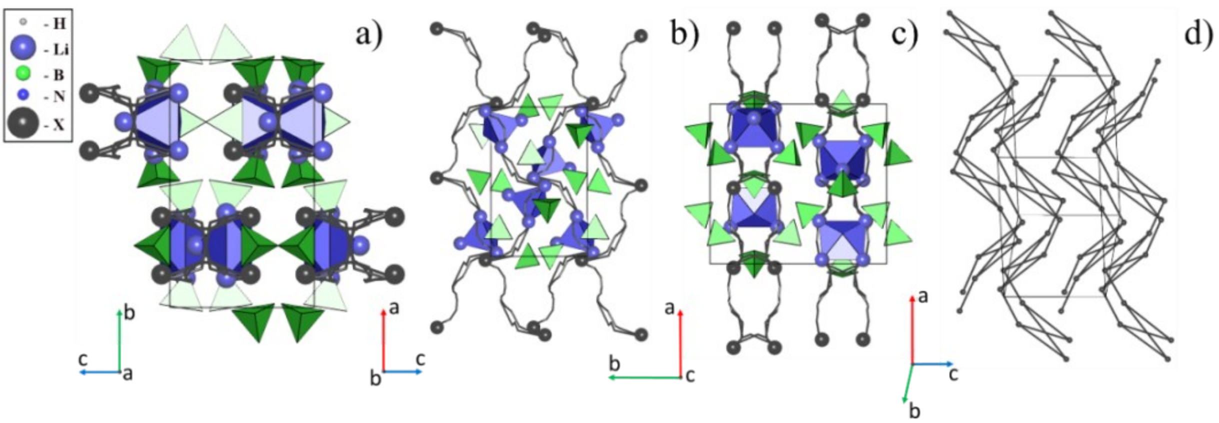

Figure S14. *a)-c) The lowest energy one-periodic Li^{+} migration map in the $Li_5(BH_4)_3NH$ structure, d) the simplified migration map of the $6^3(0,2)$ topology.*

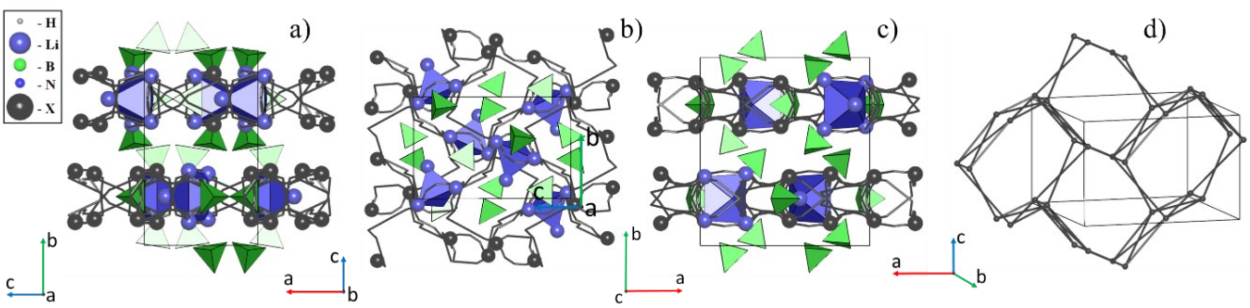

Figure S15. *a)-c) The lowest energy two-periodic Li^{+} migration map in the $Li_5(BH_4)_3NH$ structure, d) the simplified migration map with an unknown topology.*

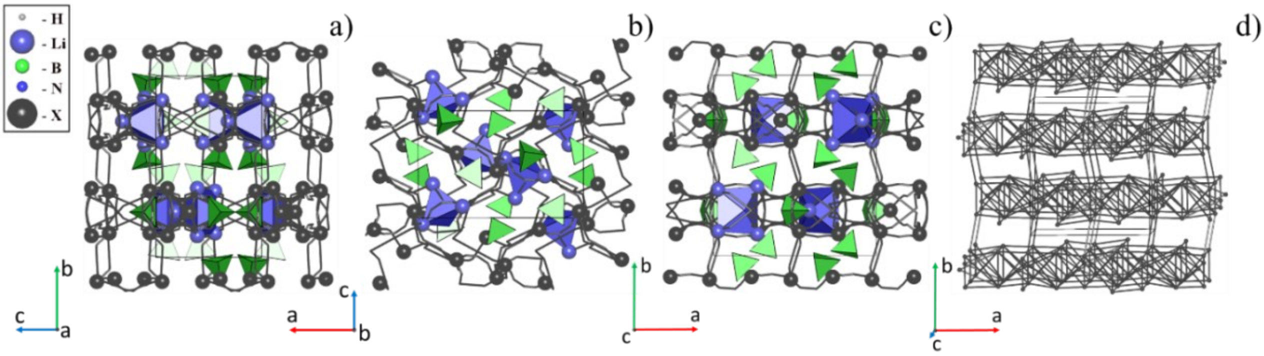

Figure S16. *a)-c) The lowest energy three-periodic Li^{+} migration map in the $Li_5(BH_4)_3NH$ structure, d) the simplified migration map with an unknown topology.*

Statistical analysis of literature data of Li-ion conductivity in $LiBH_4$

A statistical analysis was performed in order to obtain the average value of activation energy (E_A), $\ln\sigma_0$ and Li-ion conductivity at room temperature for $LiBH_4$, using literature data.[6–14] Only data related to the orthorhombic phase stable at room temperature have been considered.

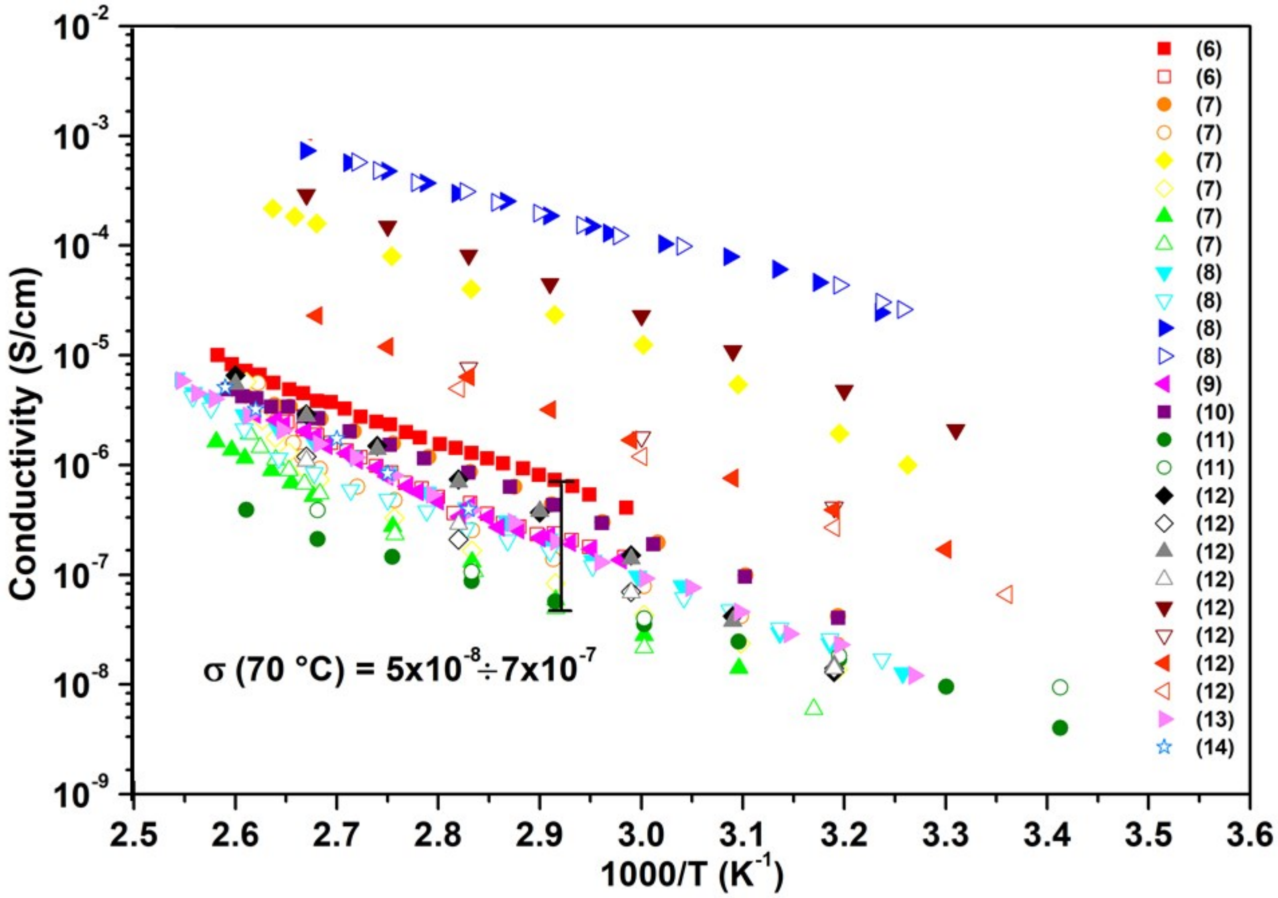

Figure S17. *Li-ion conductivity data for orthorhombic $LiBH_4$ reported in literature. Full and empty symbols refer to the heating and cooling temperature-dependent EIS ramp, respectively. The error bar for the Li-ion conductivity at 70 °C is indicated as an example.*

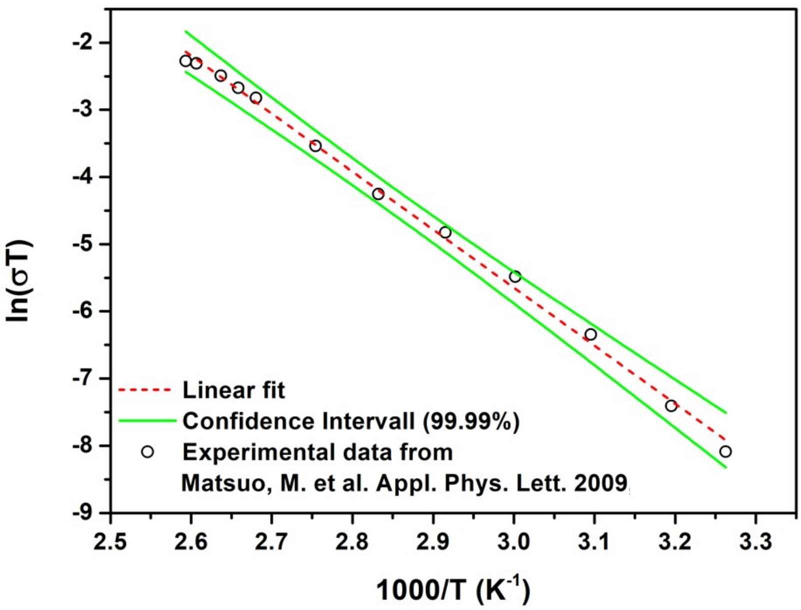

Figure S18. *Example of linear fit on Li-ion conductivity for the orthorombic phase of* $LiBH_4$ *as a function of inverse temperature. Data form Matsuo, M. et al. Appl. Phys. Lett.* ***2009****, 94, 224103 (Ref. 6).*

Temperature-dependent EIS ramp	Temperature-dependent EIS cycle	Milled	E_A (eV)	C.I.	Ref.
Heating	1st	No	0.69	0.04	(1)
Cooling	1st	No	0.81	0.09	(1)
Heating	1st	No	0.71	0.04	(2)
Cooling	1st	No	0.7	0.1	(2)
Heating	1st	**Yes**	**0.74**	**0.07**	(2)
Cooling	1st	**Yes**	**0.7**	**0.3**	(2)
Heating	2nd	**Yes**	**0.8**	**0.1**	(2)
Cooling	2nd	**Yes**	**0.9**	**0.2**	(3)
Heating	1st	No	0.77	0.04	(3)
Cooling	1st	No	0.7	0.1	(3)
Heating	1st	**Yes**	**0.51**	**0.07**	(3)
Cooling	1st	**Yes**	**0.51**	**0.05**	(3)
Heating	1st	No	0.8	0.1	(4)
Heating	1st	No	0.71	0.04	(5)
Heating	1st	No	0.50	0.1	(6)
Heating	1st	No	0.91	0.08	(7)
Heating	2nd	No	0.89	0.06	(7)
Heating	1st	**Yes**	**0.70**	**0.03**	(7)
Heating	2nd	**Yes**	**0.75**	**0.04**	(7)
Heating	1st	No	0.76	0.04	(8)
Average			**0.73**	**0.08**	
Average exclude bold data			**0.75**	**0.07**	

Table S2. *Activation energy (eV) calculated by linear plot of ln(σT) and 1000/T of literature data, for* $LiBH_4$ *(99.99 % of confidence). CI is the confidence interval half width. The bold (red) data were excluded in the second calculation of the average activation energy data. 1st and 2nd refers to the temperature-dependent EIS cycle data.*

Temperature-dependent EIS ramp	Temperature-dependent EIS cycle	Milled	lnσ_0	C.I.	Ref.
Heating	1st	No	15	1	(1)
Cooling	1st	No	18	3	(1)
Heating	1st	No	15	1	(2)
Cooling	1st	No	13	5	(2)
Heating	1st	**Yes**	**20**	**2**	(2)
Cooling	1st	**Yes**	**14**	**10**	(2)
Heating	2nd	**Yes**	**17**	**3**	(2)
Cooling	2nd	**Yes**	**20**	**8**	(3)
Heating	1st	No	16	1	(3)
Cooling	1st	No	14	4	(3)
Heating	1st	**Yes**	**15**	**2**	(3)
Cooling	1st	**Yes**	**14**	**2**	(3)
Heating	1st	No	18	3	(4)
Heating	1st	No	15	1	(5)
Heating	1st	No	6	4	(6)
Heating	1st	No	21	2	(7)
Heating	2nd	No	22	2	(7)
Heating	1st	**Yes**	**19.3**	**0.3**	(7)
Heating	2nd	**Yes**	**17**	**1**	(7)
Heating	1st	No	16	1	(8)
Average			**16**	**3**	
Average exclude bold data			**16**	**2**	

Table S3. *lnσ_0 calculated by linear plot of ln(σT) and 1000/T of literature data, for $LiBH_4$ (99.99 % of confidence). CI is the confidence interval half width. The bold (red) data were excluded in the second calculation of the average lnσ_0. 1st and 2nd refers to the temperature-dependent EIS cycle data.*

Temperature-dependent EIS ramp	Temperature-dependent EIS cycle	Milled	ln(*σT*)$_{FIT}$	ln(*σT*)$_{MAX}$	ln(*σT*)$_{MIN}$	Ref.
Heating	1st	No	-11.40	-11.18	-11.63	(1)
Cooling	1st	No	-13.12	-12.59	-13.66	(1)
Heating	1st	No	-11.98	-11.78	-12.19	(2)
Cooling	1st	No	-12.78	-13.93	-11.63	(2)
Heating	1st	**Yes**	**-8.23**	**-7.85**	**-8.61**	(2)
Cooling	1st	**Yes**	**-13.48**	**-12.12**	**-14.84**	(2)
Heating	2nd	**Yes**	**-14.41**	**-13.80**	**-15.02**	(2)
Cooling	2nd	**Yes**	**-14.90**	**-13.49**	**-16.30**	(3)
Heating	1st	No	-12.95	-12.74	-13.16	(3)
Cooling	1st	No	-12.83	-12.23	-13.43	(3)
Heating	1st	**Yes**	**-5.04**	**-4.77**	**-5.31**	(3)
Cooling	1st	**Yes**	**-5.01**	**-4.82**	**-5.20**	(3)
Heating	1st	No	-13.17	-12.53	-13.81	(4)
Heating	1st	No	-12.01	-11.81	-12.21	(5)
Heating	1st	No	-12.90	-12.53	-13.26	(6)
Heating	1st	No	-13.31	-13.04	-13.58	(7)
Heating	2nd	No	-13.72	-13.44	-13.99	(7)
Heating	1st	**Yes**	**-7.25**	**-6.36**	**-8.13**	(7)
Heating	2nd	**Yes**	**-11.81**	**-11.24**	**-12.37**	(7)
Heating	1st	No	-12.90	-12.68	-13.12	(8)
Average ln(*σT*)			**-11.66**	**-11.25**	**-12.07**	**C.I.**
Average *σ* at 30 °C			**2.85x10^{-8}**	**4.30x10^{-8}**	**1.89x10^{-8}**	**1.21x10^{-8}**
Average ln(*σT*) exclude bold data			**-12.76**	**-12,54**	**-12,97**	**C.I.**
Average *σ* at 30 °C exclude bold data			**9.5x10^{-9}**	**1.18x10^{-8}**	**7.66x10^{-9}**	**2.07x10^{-9}**

Table S4. *ln(σT) and Li-ion conductivity at 30 °C (303.14 K) calculated using the data (1000 E_A/k_B and $ln\sigma_0$) obtained by the linear plot of ln(σT) and 1000/T of literature data (see Table S1 and Table S2) for $LiBH_4$. ln(σT)$_{FIT}$ has been calculated using the slope and intercept obtained by the linear fit. ln(σT)$_{MAX}$ and ln(σT)$_{MIN}$ were calculated considering the maximum and the minimum values, of the slope and intercept, of confidence interval obtained by the linear fit. The bold (red) data were excluded in the second calculation of the average ln(σT) data. 1st and 2nd refers to the temperature-dependent EIS cycle data. CI is the confidence interval half width, calculated averaging the ln(σT)$_{MAX}$ and the ln(σT)$_{MIN}$.*

Statistical analysis for $LiNH_2$, Li_2NH, $Li_2(NH_2)(BH_4)$ and $Li_4(NH_2)_3(BH_4)$

Statistical analysis was performed in order to obtain the average value of activation energy for $LiNH_2$, Li_2NH, $Li_2(NH_2)(BH_4)$ and $Li_4(NH_2)_3(BH_4)$, using the data reported in literature.[10,15–18]

Compound	Temperature-dependent EIS ramp	Temperature-dependent EIS cycle	E_A	C.I.	$\ln\sigma_0$	C.I.	Ref.
$LiNH_2$	Heating	1st	0.9	0.04	19	1	(10)
	Heating	1st	1.05	0.08	19	2	(11)
	Average		**0.98**	**0.06**	**19**	**2**	
Li_2NH	Heating	1st	0.63	0.01	21.8	0.2	(11)
	Heating	1st	0.58	0.02	20,1	0,9	(12)
	Heating	1st	0.6	0.1	20	5	(12)
	Average		**0.60**	**0.04**	**21**	**2**	
$Li_2NH_2BH_4$	Heating	1st	0.7	0.04	23	1	(10)
	Cooling	1st	0.67	0.06	22	2	(10)
	Average		**0.69**	**0.06**	**23**	**2**	
$Li_4(NH_2)_3BH_4$	Heating	1st	0.26	0.01	7,0	0,4	(5)
	Heating	1st	0.33	0.01	8.7	0.4	(10)
	Cooling	1st	0.55	0.03	13	1	(10)
	Heating	1st	0.34	0.01	11	1	(13)
	Average		**0.37**	**0.02**	**10.1**	**0.6**	

Table S5. *Activation energy (eV) and $\ln\sigma_0$ calculated by linear plot of $\ln(\sigma T)$ and 1000/T of literature data, for the $LiNH_2$, Li_2NH, $Li_2(NH_2)(BH_4)$ and $Li_4(NH_2)_3(BH_4)$ (95 % of confidence). CI is the confidence interval half width.*

Compound	Temperature-dependent EIS ramp	Temperature-dependent EIS cycle	**ln(*σT*)$_{FIT}$**	**ln(*σT*)$_{MAX}$**	**ln(*σT*)$_{MIN}$**	**Ref.**
$LiNH_2$	Heating	1st	-14.97	-14.71	-15.23	(5)(10)
	Heating	1st	-20.90	-19.75	-22.05	(11)
	Average ln(*σT*)		**-17.94**	**-17.23**	**-18.64**	**C.I.**
	Average *σ* at 30 °C		**$5.36x10^{-11}$**	**$1.09x10^{-10}$**	**$2.64x10^{-11}$**	**$4.11x10^{-11}$**
Li_2NH	Heating	1st	-2.41	-2,38	-2,44	11
	Heating	1st	-2.22	-2,17	-2,27	12
	Heating	1st	-1.96	-1,32	-2,61	12
	Average ln(*σT*)		**-2.20**	**-1,96**	**-2,44**	**C.I.**
	Average *σ* at 30 °C		**$3.66x10^{-4}$**	**$4.66x10^{-4}$**	**$2.88x10^{-4}$**	**$8.92x10^{-5}$**
$Li_2NH_2BH_4$	Heating	1st	-3.36	-3.22	-3.50	(5)(10)
	Cooling	1st	-3.62	-3.43	-3.80	(10)
	Average ln(*σT*)		**-3.49**	**-3.33**	**-3.65**	**C.I.**
	Average *σ* at 30 °C		**$1.01x10^{-4}$**	**$1.18x10^{-4}$**	**$8.57x10^{-5}$**	**$1.63x10^{-5}$**
$Li_4(NH_2)_3BH_4$	Heating	1st	-2.93	-2.86	-3.00	(5)
	Heating	1st	-3.53	-3.44	-3.62	(10)
	Cooling	**1st**	**-7.59**	**-7.39**	**-7.79**	(10)
	Heating	1st	-2.74	-2.11	-3.37	(13)
	Average ln(*σT*)		**-4.19**	**-3.95**	**-4.44**	**C.I.**
	Average *σ* at 30 °C		**$4.98x10^{-5}$**	**$6.37x10^{-5}$**	**$3.89x10^{-5}$**	**$1.24x10^{-5}$**
	Average ln(*σT*) exclude bold data		**-3,06**	**-2.80**	**-3.33**	**C.I.**
	Average *σ* at 30 °C exclude bold data		**$1.54x10^{-4}$**	**$2.00x10^{-4}$**	**$1.14x10^{-4}$**	**$4.09x10^{-5}$**

Table S6. *ln(σT) and Li-ion conductivity at 30 °C (303.14 K) calculated using the data (1000 E_A/k_B and lnσ_0) obtained by the linear plot of ln(σT) and 1000/T of literature data (see Table S1 and Table S2) for the $LiNH_2$, Li_2NH, $Li_2(NH_2)(BH_4)$ and $Li_4(NH_2)_3(BH_4)$. ln(σT)$_{FIT}$ has been calculated using the slope and intercept obtained by the linear fit. ln(σT)$_{MAX}$ and ln(σT)$_{MIN}$ were calculated considering the maximum and the minimum values, of the slope and intercept, of confidence interval obtained by the linear fit. The bold (red) data were excluded in the second calculation of the average ln(σT) data. 1st and 2nd refers to the temperature-dependent EIS cycle data. CI is the confidence interval half width, calculated averaging the maximum and the ln(σT)$_{MAX}$ and the ln(σT)$_{MIN}$.*

References

(1) Soulie, J.; Renaudin, G.; Černý, R.; Yvon, K. Lithium Boro-Hydride $LiBH_4$ I. Crystal Structure. *J. Alloys Compd.* 2002, **346**, 200–205.

(2) Noritake, T.; Nozaki, H.; Aoki, M.; Towata, S.; Kitahara, G.; Nakamori, Y.; Orimo, S. Crystal Structure and Charge Density Analysis of Li_2NH by Synchrotron X-Ray Diffraction. *J. Alloys Compd.* 2005, **393**, 264–268.

(3) Yang, J. B.; Zhou, X. D.; Cai, Q.; James, W. J.; Yelon, W. B. Crystal and Electronic Structures of $LiNH_2$. *Appl. Phys. Lett.* 2006, **88**, 041914.

(4) Noritake, T.; Aoki, M.; Towata, S.; Ninomiya, A.; Nakamori, Y.; Orimo, S. Crystal Structure Analysis of Novel Complex Hydrides Formed by the Combination of $LiBH_4$ and $LiNH_2$. *Appl. Phys. A* 2006, **83**, 277–279.

(5) Wolczyk, A.; Paik, B.; Sato, T.; Nervi, C.; Brighi, M.; GharibDoust, S. P.; Chierotti, M.; Matsuo, M.; Li, G.; Gobetto, R.; Jensen, T. R.; Černý, R.; Orimo, S.; Baricco, M. $Li_5(BH_4)_3NH$: Lithium-Rich Mixed Anion Complex Hydride. *J. Phys. Chem. C* 2017, **121**, 11069–11075.

(6) Matsuo, M.; Nakamori, Y.; Orimo, S.; Maekawa, H.; Takamura, H. Lithium Superionic Conduction in Lithium Borohydride Accompanied by Structural Transition. *Appl. Phys. Lett.* 2007, **91**, 224103.

(7) Matsuo, M.; Takamura, H.; Maekawa, H.; Li, H.-W.; Orimo, S. Stabilization of Lithium Superionic Conduction Phase and Enhancement of Conductivity of $LiBH_4$ by LiCl Addition. *Appl. Phys. Lett.* 2009, **94**, 084103.

(8) Sveinbjörnsson, D.; Blanchard, D.; Myrdal, J. S. G.; Younesi, R.; Viskinde, R.; Riktor, M. D.; Norby, P.; Vegge, T. Ionic Conductivity and the Formation of Cubic CaH_2 in the $LiBH_4$–$Ca(BH_4)_2$ Composite. *J. Solid State Chem.* 2014, **211**, 81–89.

(9) Miyazaki, R.; Karahashi, T.; Kumatani, N.; Noda, Y.; Ando, M.; Takamura, H.; Matsuo, M.; Orimo, S.; Maekawa, H. Room Temperature Lithium Fast-Ion Conduction and Phase Relationship of LiI Stabilized $LiBH_4$. *Solid State Ionics* 2011, **192**, 143–147.

(10) Matsuo, M.; Remhof, A.; Martelli, P.; Caputo, R.; Ernst, M.; Miura, Y.; Sato, T.; Oguchi, H.; Maekawa, H.; Takamura, H.; et al. Complex Hydrides with $(BH_4)^-$ and $(NH_2)^-$ Anions as New Lithium Fast-Ion Conductors. *J. Am. Chem. Soc.* 2009, **131**, 16389–16391.

(11) Gulino, V.; Brighi, M.; Dematteis, E. M.; Murgia, F.; Nervi, C.; Černý, R.; Baricco, M. Phase Stability and Fast Ion Conductivity in the Hexagonal $LiBH_4$–LiBr–LiCl Solid Solution. *Chem. Mater.* 2019, **31**, 5133–5144.

(12) Gulino, V.; Barberis, L.; Ngene, P.; Baricco, M.; de Jongh, P. E. Enhancing Li-Ion Conductivity in $LiBH_4$-Based Solid Electrolytes by Adding Various Nanosized Oxides. *ACS*

Appl. Energy Mater. 2020, **3**, 4941–4948.

(13) Blanchard, D.; Nale, A.; Sveinbjörnsson, D.; Eggenhuisen, T. M.; Verkuijlen, M. H. W.; Suwarno; Vegge, T.; Kentgens, A. P. M.; de Jongh, P. E. Nanoconfined $LiBH_4$ as a Fast Lithium Ion Conductor. *Adv. Funct. Mater.* 2015, **25**, 184–192.

(14) Choi, Y. S.; Lee, Y.-S.; Oh, K. H.; Cho, Y. W. Interface-Enhanced Li Ion Conduction in a $LiBH_4$–SiO_2 Solid Electrolyte. *Phys. Chem. Chem. Phys.* 2016, **18**, 22540–22547.

(15) Zhou, Y.; Matsuo, M.; Miura, Y.; Takamura, H.; Maekawa, H.; Remhof, A.; Borgschulte, A.; Zuttel, A.; Otomo, T.; Orimo, S. Enhanced Electrical Conductivities of Complex Hydrides $Li_2(BH_4)(NH_2)$ and $Li_4(BH_4)(NH_2)_3$ by Melting. *Mater. Trans.* 2011, **52**, 654–657.

(16) Li, W.; Wu, G.; Xiong, Z.; Feng, Y. P.; Chen, P. Li^+ Ionic Conductivities and Diffusion Mechanisms in Li-Based Imides and Lithium Amide. *Phys. Chem. Chem. Phys.* 2012, **14**, 1596–1606.

(17) Boukamp, B. A.; Huggins, R. A. Ionic Conductivity in Lithium Imide. *Phys. Lett. A* 1979, **72**, 464–466.

(18) Yan, Y.; Kühnel, R.-S.; Remhof, A.; Duchêne, L.; Reyes, E. C.; Rentsch, D.; Łodziana, Z.; Battaglia, C. A Lithium Amide-Borohydride Solid-State Electrolyte with Lithium-Ion Conductivities Comparable to Liquid Electrolytes. *Adv. Energy Mater.* 2017, **7**, 1700294.